Insights into the structure, function and evolution of the radical-SAM 23S rRNA methyltransferase Cfr that confers antibiotic resistance in bacteria

Karminska, K. H.; Purta, E.; Hansen, L .H.; Bujnicki, J. M.; Vester, B.; Long, Katherine

Published in:
Nucleic Acids Research

Link to article, DOI:
10.1093/nar/gkp1142

Publication date:
2010

Document Version
Publisher's PDF, also known as Version of record

1652–1663 *Nucleic Acids Research, 2010, Vol. 38, No. 5* *Published online 10 December 2009*
doi:10.1093/nar/gkp1142

Insights into the structure, function and evolution of the radical-SAM 23S rRNA methyltransferase Cfr that confers antibiotic resistance in bacteria

Katarzyna H. Kaminska[1], Elzbieta Purta[1], Lykke H. Hansen[2], Janusz M. Bujnicki[1,3,*], Birte Vester[2,*] and Katherine S. Long[4,*]

[1]Laboratory of Bioinformatics and Protein Engineering, International Institute of Molecular and Cell Biology, Trojdena 4, 02-109 Warsaw, Poland, [2]Department of Biochemistry and Molecular Biology, University of Southern Denmark, Campusvej 55, DK-5230 Odense M, Denmark, [3]Institute for Molecular Biology and Biotechnology, Adam Mickiewicz University, Umultowska 89, PL-61-614 Poznan, Poland and [4]Department of Biology, University of Copenhagen, Copenhagen Biocenter, Ole Maaløes Vej 5, DK-2200 Copenhagen N, Denmark

Received August 6, 2009; Revised and Accepted November 18, 2009

ABSTRACT

The Cfr methyltransferase confers combined resistance to five classes of antibiotics that bind to the peptidyl tranferase center of bacterial ribosomes by catalyzing methylation of the C-8 position of 23S rRNA nucleotide A2503. The same nucleotide is targeted by the housekeeping methyltransferase RlmN that methylates the C-2 position. Database searches with the Cfr sequence have revealed a large group of closely related sequences from all domains of life that contain the conserved CX_3CX_2C motif characteristic of radical *S*-adenosyl-L-methionine (SAM) enzymes. Phylogenetic analysis of the Cfr/RlmN family suggests that the RlmN subfamily is likely the ancestral form, whereas the Cfr subfamily arose via duplication and horizontal gene transfer. A structural model of Cfr has been calculated and used as a guide for alanine mutagenesis studies that corroborate the model-based predictions of a 4Fe–4S cluster, a SAM molecule coordinated to the iron–sulfur cluster (SAM1) and a SAM molecule that is the putative methyl group donor (SAM2). All mutations at predicted functional sites affect Cfr activity significantly as assayed by antibiotic susceptibility testing and primer extension analysis. The investigation has identified essential amino acids and Cfr variants with altered reaction mechanisms and represents a first step towards understanding the structural basis of Cfr activity.

INTRODUCTION

The *cfr* gene was originally identified as a chloramphenicol–florfenicol resistance determinant on a multiresistance plasmid isolated during a surveillance study of florfenicol resistance among staphylococci from animals (1). It was subsequently shown to encode an rRNA methyltransferase (MTase) that targets nucleotide A2503 of *Escherichia coli* 23S rRNA (2). Antimicrobial susceptibility testing of *E. coli* and *Staphylococcus aureus* strains expressing the Cfr MTase revealed that these strains exhibit combined resistance to a number of chemically unrelated drugs that bind to overlapping sites that abut nucleotide A2503 at the ribosomal peptidyl transferase center (2,3). The phenotype was named $PhLOPS_A$ for resistance to the following drug classes: Phenicols, Lincosamides, Oxazolidinones, Pleuromutilins, and Streptogramin A antibiotics (3). It is also known that Cfr expression confers resistance to the 16-membered macrolides josamycin and spiramycin (4). Thus, the Cfr-mediated resistance functions in both Gram-positive and -negative bacteria and includes important antimicrobial agents that are currently used in human and/or veterinary medicine. The detection of *cfr* on plasmids and transposons raises concerns about spreading of Cfr-mediated resistance (5).

In a recent study, the specific identity of the Cfr-mediated methylation at nucleotide A2503 of 23S rRNA was determined to be 8-methyladenosine, a hitherto undescribed modification in natural RNA molecules (6). It was also revealed that Cfr has a less pronounced ability to catalyze methylation at position C-2 of A2503 to form

*To whom correspondence should be addressed. Tel: +48 22 597 0750; Fax: +48 22 597 0715; Email: iamb@genesilico.pl
Correspondence may also be addressed to Birte Vester. Tel: +45 65 50 23 77; Fax: +45 65 50 24 67; Email: b.vester@bmb.sdu.dk
Correspondence may also be addressed to Katherine S. Long. Tel: +45 35 32 20 42; Fax: +45 35 23 21 28; Email: long@bio.ku.dk

2,8-dimethyladenosine. The antibiotic resistance conferred by Cfr is provided by methylation at position C-8 and is independent of methylation at position C-2 (6). In *E. coli*, there is a natural m^2A methylation at A2503 (7) that is mediated by the RlmN MTase (8). This methylation is considered to be a housekeeping modification rather than a genuine antibiotic resistance determinant, as lack of the methylation only causes a slight increase in susceptibility to hygromycin A, linezolid, sparsomycin and tiamulin (8).

The sequences of Cfr and RlmN are similar to each other but show no significant similarity to other known enzymes involved in resistance against the above-mentioned antibiotics or to any known MTases. However, multiple sequence alignments of the Cfr/RlmN family (1,8) have revealed a cysteine-rich motif similar to a catalytic motif of radical-*S*-adenosyl-L-methionine (SAM) enzymes (9,10). Radical-SAM enzymes contain a $[4Fe–4S]^+$ cluster that is coordinated by the three conserved cysteine thiolate side chains in the CX_3CX_2C motif and one molecule of SAM (10). The reactions catalyzed by radical-SAM enzymes are diverse, but their mechanisms all involve the cleavage of unreactive C–H bonds by a 5′-deoxyadenosyl radical generated by reductive cleavage of SAM (10). The mutation of single conserved cysteines in the CX_3CX_2C motif of Cfr abolishes its activity, lending support to the idea that the Cfr modification reaction occurs via a radical-based mechanism (6).

In this study, bioinformatics analysis of the Cfr/RlmN family for the first time establishes their significant evolutionary link with radical-SAM enzymes. Also, a structural model of Cfr was built using theoretical protein structure prediction methods to guide the investigation of sequence–function relationships. Finally, mutagenesis of selected single residues in Cfr and functional analysis of the mutant proteins has identified essential amino acids and supports the predictions of ligand binding sites.

MATERIALS AND METHODS

Sequence analysis

Searches of the current version of non-redundant sequence database (nr) were carried out using a local version of PSI-BLAST (11) with *E*-value threshold of 0.001, until convergence. All sequences were extracted and a preliminary alignment was calculated using MUSCLE (12) with default parameters and a preliminary tree was calculated using the neighbor-joining approach implemented in MEGA4 (13). Incomplete sequences and alternative versions of the same protein from the same species were removed. Finally, the multiple sequence alignment was refined manually to ensure that no unwarranted gaps had been introduced within α-helices and β-strands. A phylogenetic tree was calculated with MEGA4 (13) using the minimum evolution (ME) method, with the JTT model of substitutions and pairwise deletions, and the initial tree calculated by the ME method with the Closest Neighbor Search option set to level = 2. The stability of individual nodes was calculated using the bootstrap test (1000 replicates) to judge the strength of statistical support for nodes on phylogenetic trees. The number presented by each node reflects the percentage of bootstrap trees that resolve a given clade. Additionally, the statistical support for each node was confirmed by the Interior Branch Test (ITB) in all trees (1000 replicates). For all branches with bootstrap support >50%, the ITB support was equal or higher (data not shown).

Protein fold recognition: identification of domains and templates

Secondary structure prediction and tertiary fold-recognition (FR) were carried out via the GeneSilico MetaServer (14), (http://genesilico.pl/meta2/ for details). Based on the coverage of the query sequence by potential template domains detected by FR, two independently folded domains in the query protein sequence were identified, and the corresponding sequence fragments (aa 1–102 and 103–312) and the remaining C-terminal extension (aa 313–349) were submitted to the MetaServer as additional independent queries. FR alignments between the query sequence and its fragments were compared, evaluated, and ranked by the Pcons method (15).

Protein structure modeling

Models of individual domains in the query sequence were constructed based on the FR results using the so-called 'FRankenstein's Monster' approach (16,17). The most up-to-date version of this protocol involves iterative model building by MODELLER (18), evaluation by MetaMQAP (see below for a more detailed explanation), realignment in poorly scored regions and merging of best-scoring fragments. The conformations of the N-terminus (aa 1–102) and the C-terminus (aa 313–349) were modeled *de novo* with the ROSETTA method for template-free modeling of protein structure (19), and the resulting models were optimized with REFINER (20).

Protein model evaluation and structure analysis

The predicted accuracy of modeled structures (i.e. their expected agreement with the true structures that are unknown) was calculated with the model quality assessment programs (MQAPs) MetaMQAP (21) and PROQ (22). MQAPs work best with single domains and are usually incapable of predicting the accuracy of mutual positions of domains. MQAPs merely predict the deviation of a model from the real structure, as a real deviation can only be calculated if the real structure is known. Thus, scores that indicate e.g. 'very good models', must be interpreted as estimations or predictions that our models are 'very good', and not as ultimate validation of the model quality.

Models and their features were visualized with PyMOL (23). Mapping of the electrostatic potential on protein surfaces was done with Adaptive Poisson-Boltzmann Solver (APBS) (24). Mapping of sequence conservation on protein surfaces was done with COLORADO3D (25) and CONSURF (26).

Bacterial strains and growth conditions

Escherichia coli strains were grown in LB medium using standard procedures (27) and in the presence of 100 μg/ml ampicillin where appropriate for plasmid selection and maintenance. The hyperpermeable strain AS19 (28) was transformed with plasmid-borne *cfr* genes (wt and mutated genes) and used for antibiotic susceptibility testing. The 'Keio' collection strain JW2501-1 (29), where the *rlmN* (*yfgB*) gene is replaced with a kanamycin resistance cassette, was also transformed with plasmid-borne *cfr* genes (wt and mutated genes) and used for isolation of RNA for primer extension analysis.

Cloning of *cfr* and construction of plasmids encoding Cfr mutant proteins

The *cfr* gene was amplified by PCR using the upstream primer 5′-GCGCATTGCATATGCATCACCATCAC CATCACAAAGAAATGAATTTTAATAATAAA-3′ encoding a N-terminal histidine affinity tag and the downstream primer 5′-CATAGCAAGCTTCTATTGGCTATT TTGATAATTAC-3′. The plasmid pBglII (Cfr+) (2) containing the *cfr* gene cloned into the pBluescript II SK+ vector (Stratagene) was used as a template in the PCR amplification. The tagged *cfr* gene was brought under control of the *lac* promoter by insertion into the NdeI and HindIII sites in plasmid pLJ102 (30) to form plasmid pCfrHis. The pCfrHis plasmids encoding Cfr mutants containing a single amino acid to alanine mutation at residues R25, Q28, E91, C105, C110, C112, C116, F118, C119, S189, S212, H214 and C338 were constructed in two steps using overlap extension PCR (27). First, two overlapping fragments were amplified with an outer primer complementary to sequences flanking the 5′ or 3′ end of the *cfr* gene and a mutagenic primer in the opposite orientation introducing the appropriate mutations (Supplementary Table S1). The two outer primers were then used to amplify fragments containing full-length mutant *cfr* genes, with the two overlapping fragments from the first step used as the template (Supplementary Table S1). The fragments were cloned into the NdeI and HindIII sites of plasmid pLJ102 to form the pCfrHis plasmids. The plasmids were sequenced to confirm the presence of the mutations and then used to transform *E. coli* strains AS19 and JW2501-1.

Antibiotic susceptibility testing

Drug susceptibility testing was done in a microtiter plate format by measuring optical density values at 450 nm with a microtiter plate reader (Victor 3, Perkin Elmer). LB medium was inoculated with single colonies and incubated overnight at 37°C. The cultures were diluted to OD_{450} = 0.01 and 100 μl diluted culture was mixed with 100 μl of antibiotic solutions in water in a series with 2-fold concentration steps and all strains were induced by addition of 1 mM IPTG. The tested concentration ranges were: florfenicol 0.25–32 μg/ml and tiamulin 0.5–128 μg/ml. The minimal inhibitory concentration (MIC) was defined as the lowest tested drug concentration at which the growth of the cultures was completely inhibited after 48 h of incubation at 37°C. Although reproducible 2-fold differences in MICs do not represent large changes in antibiotic susceptibility, they can nevertheless represent measurable small changes in activity.

Primer extension analysis

For RNA isolation, overnight cultures were diluted into LB medium supplemented with 100 μg/ml ampicillin and incubated with shaking at 37°C. After 45 min, the cultures were induced with 1 mM IPTG and incubated until OD_{450} reached 0.5. Total RNA was isolated with the RNeasy kit (Qiagen). For isolation of ribosomal RNA, cells were harvested, washed with TMN buffer (50 mM Tris–HCl at pH 7.8, 10 mM $MgCl_2$, 100 mM NH_4Cl) and resuspended in TMN. The cells were then lysed by sonication, followed by removal of cell debris by centrifugation. The supernatants were loaded on 10–40% sucrose gradients in TMN and subjected to ultracentrifugation in the swinging bucket rotor AH629 (18 000 r.p.m., 19 h, 4°C). The 70S fractions (and for Cfr mutant C105A also the 50S fractions) were collected and dialysed against TMN. Finally, the 70S ribosomes were pelleted by ultracentrifugation in a Ti 50 rotor (40 000 r.p.m., 24 h, 4°C) and dissolved in TMN. Following phenol extraction of 70S ribosomes, ribosomal RNA was precipitated with ethanol, and resuspended in water.

Modification of ribosomal RNA was monitored by primer extension analysis (31) with AMV reverse transcriptase (Finnzymes). The 5′-[^{32}P]-labeled deoxyoligonucleotide primer (5′-GAACAGCCATACCCTTG-3′), complementary to nucleotides 2540–2556 of *E. coli* 23S rRNA was used. The cDNA extension products were separated on 6% polyacrylamide sequencing gels. The positions of the stops were visualized by autoradiography and identified by referencing to dideoxynucleotide sequencing reactions on 23S rRNA that were electrophoresed in parallel.

RESULTS

Sequence analysis and phylogeny of the Cfr/RlmN family

To address the question of whether Cfr is a true member of the radical-SAM superfamily, a comprehensive bioinformatics analysis of Cfr, RlmN and other known radical-SAM enzymes was carried out. Sequence database searches with the Cfr sequence as a query against the nr database led to the identification of a large family of 731 closely related sequences from all three domains of life and from viruses. Figure 1 shows a multiple sequence alignment of selected Cfr/RlmN members and the complete alignment is available as Supplementary Data. The conserved CX_3CX_2C motif is present in all members with the sole exception of an uncharacterized protein from *Ureaplasma parvum* (GI 13357773) that is likely to be an enzymatically inactive member of the Cfr/RlmN family.

In order to elucidate the phylogenetic relationships of the Cfr/RlmN family we have calculated the Minimum Evolution phylogenetic tree based on the complete

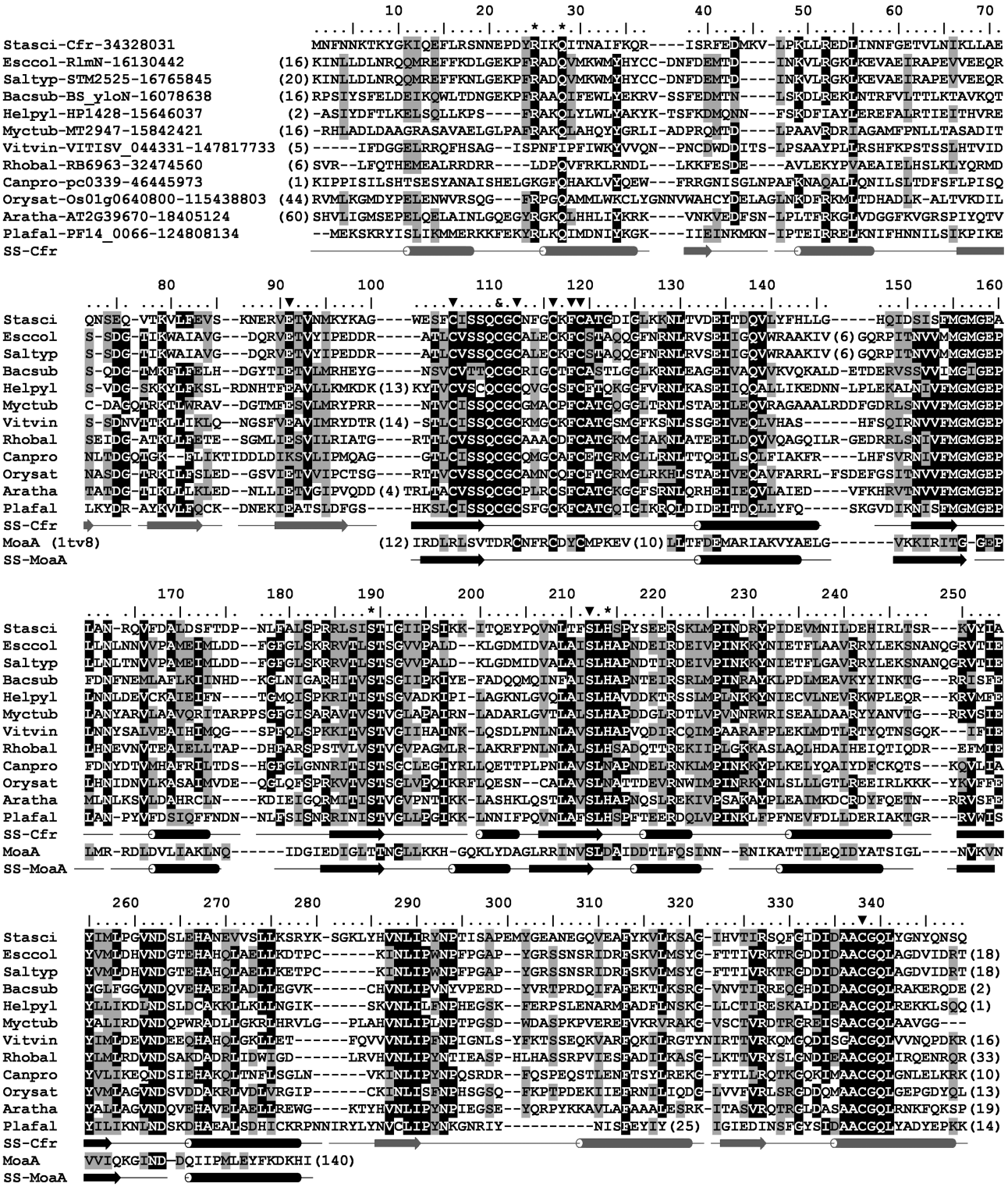

Figure 1. Multiple alignment of representative members of the Cfr/RlmN family. The sequences represent members of major phyla and have been selected based on phylogenetic analysis. The sequences are named using six-letter abbreviations for genus and species, for instance: Esccol for *Escherichia coli*, followed by the gene name and the NCBI gene identification number. Residues that are conserved and physicochemically similar in >50% of the sequences are indicated by black and grey shading, respectively. Secondary-structures predicted for Cfr and observed in the template crystal structure (MoaA; PDB accession code 1tv8) are indicated as arrows (strands) and tubes (helices) at the bottom of the figure. Strands and helices are shown in black in regions modeled based on the templates, while regions folded *de novo* are shown in grey. Mutational data for Cfr are annotated above the sequence for essential (filled inverted triangles), conditional (asterisks), and non-essential (ampersand) positions.

alignment of the 731 related sequences. The tree shown in Figure 2 confirms the existence of two main subfamilies comprising Cfr and RlmN homologs, respectively, and suggests the presence of an additional small subfamily with enzymes of unknown function. The RlmN branch comprises members from most bacterial taxons and its topology generally agrees with the universally accepted taxonomy of bacteria (32). In contrast, the Cfr branch contains representatives from only a few taxons: eukaryotic (green plants, alveolates, Choanoflagellida) and bacterial (Chlamydiae/Verrucomicrobia group, Planctomycetes and Staphylococci). In the Cfr branch, the relationships of the proteins completely disagree with the taxonomy of the host organisms (e.g. proteins from the same taxon are found on different sub-branches with members from other different taxons). The data suggest that vertical transfer has governed the evolution of the RlmN while Cfr has evolved in a horizontal manner. Thus, it is likely that RlmN represents the ancestral form, while members of the Cfr family are most likely products of duplication(s) and horizontal gene transfer(s).

Cfr/RlmN-like proteins are only present in Eukaryota that contain plastids (plants and choanoflagellates) or whose ancestor is predicted to contain plastids (alveolates). They are also absent from Archaea with the exception of *Nitrosopumilus maritimus*. This suggests that the Cfr/RlmN family has a bacterial origin and other taxons acquired their members by horizontal gene transfer(s). Plants contain up to three members of the Cfr/RlmN family (e.g. AT2G39670, AT1G60230 and AT3G19630 in *Arabidopsis thaliana*), which appear to be phylogenetically associated with Cyanobacteria and Proteobacteria in the RlmN branch, and with Alveolata in the Cfr branch, respectively. Predictions of subcellular localizations with the WoLFPSORT method (33) failed to indicate any preference associated with any of the tree lineages (e.g. different members of each lineage are predicted to be targeted to different compartments). Nonetheless, the distribution of bacterial and plant members suggests a scenario in which most of bacterial members of the RlmN lineage are orthologs, direct (vertical) descendants of the ancestor of the family. The cyanobacterial RlmN has presumably been transferred to plants via the chloroplast endosymbiont. Additional horizontal transfers contributed to the emergence of these RlmN family members, whose position on the tree clearly disagrees with the organismal phylogeny (e.g. a crenarchaeal RlmN ortholog on a branch with plants and Cyanobacteria or one of the plant members on the branch comprising mostly Deltaproteobacteria). We speculate that the ancestral Cfr paralog has been created by gene duplication in a plant cell, from which it has been transferred to alveolates and bacteria, including Firmicutes (clostridia, bacilli and staphylococci). This implies that the ability of Cfr to introduce the m^8A modification is a novel feature. It will be interesting to determine whether its plant homologs also share this activity, which might provide clues as to the physiological role of Cfr and its function beyond antibiotic resistance in bacteria.

Generation and validation of a structural model of Cfr

As a starting point for a structural model of Cfr, a protein fold-recognition (FR) analysis of the Cfr sequence was performed. FR methods attempt to identify the most appropriate modeling templates for a query sequence and report a series of alignments to proteins of known structure. The analysis confirmed with a high reliability (Pcons score 2.64, with values >1 indicating a confident prediction) that Cfr contains a radical-SAM domain in the central part of the sequence (residues 103–312). Most FR methods included in the MetaServer consistently reported the structure of the radical-SAM enzyme molybdenum cofactor biosynthesis protein A (MoaA; PDB code: 1tv8) as the potentially best template for modeling of the central domain in Cfr (top six matches to MoaA, with Pcons scores 2.09–2.64). Despite the unanimous identification of the radical-SAM domain in the central part of the Cfr sequence, FR alignments by different methods showed differences, suggesting that modeling of the Cfr structure may be a challenge. In addition, a drawback of a template-based modeling procedure is the inability to model 'structurally variable regions' (SVRs, e.g. large insertions, terminal extensions, etc.) that have no counterpart in any of the templates. The Cfr sequence contains two such regions, the N-terminal region (residues 1–102) and the C-terminal region (residues 313–349). The FR analyses of the terminal regions of Cfr showed no statistically significant similarity to any structurally characterized template and therefore had to be modeled *de novo*.

A model of the central domain was constructed using the 'FRankenstein's Monster' protocol designed to overcome the lack of consensus in the FR alignments (16). As expected from comparative modeling, the central domain of Cfr revealed features of its templates, namely an α/β domain with a topology of an incomplete TIM-barrel that is characteristic for radical-SAM enzymes (34). The variable N- and C-termini were modeled *de novo* using ROSETTA and added to the homology-modeled core. Interestingly, the model of the N-terminal region shows an extension of the β-sheet in the radical-SAM domain and an additional helical domain, with a topology similar to HTH proteins, in particular the 'winged helix' (wH) superfamily (35). Thus, the N-terminal region is likely to constitute an independent domain, and it will be referred to as the N-terminal domain (NTD). The C-terminal region folded to form an extension of the other edge of the β-sheet in the radical-SAM domain, in the form of a Rossmann-like α/β/α unit, and does not appear to form an independent domain. The final model was obtained by optimization of packing with REFINER and is presented in Figure 3.

The prediction of the potential deviation of the final model, comprised of both the homology-modeled core and *de novo* folded termini, yields good scores with MQAP methods. The program PROQ predicted an LGscore of 4.163, which indicates a 'very good model', while MetaMQAP predicted that the whole model exhibits a root mean square deviation from the true structure on the order of 2.4 Å, and a predicted GDT_TS score

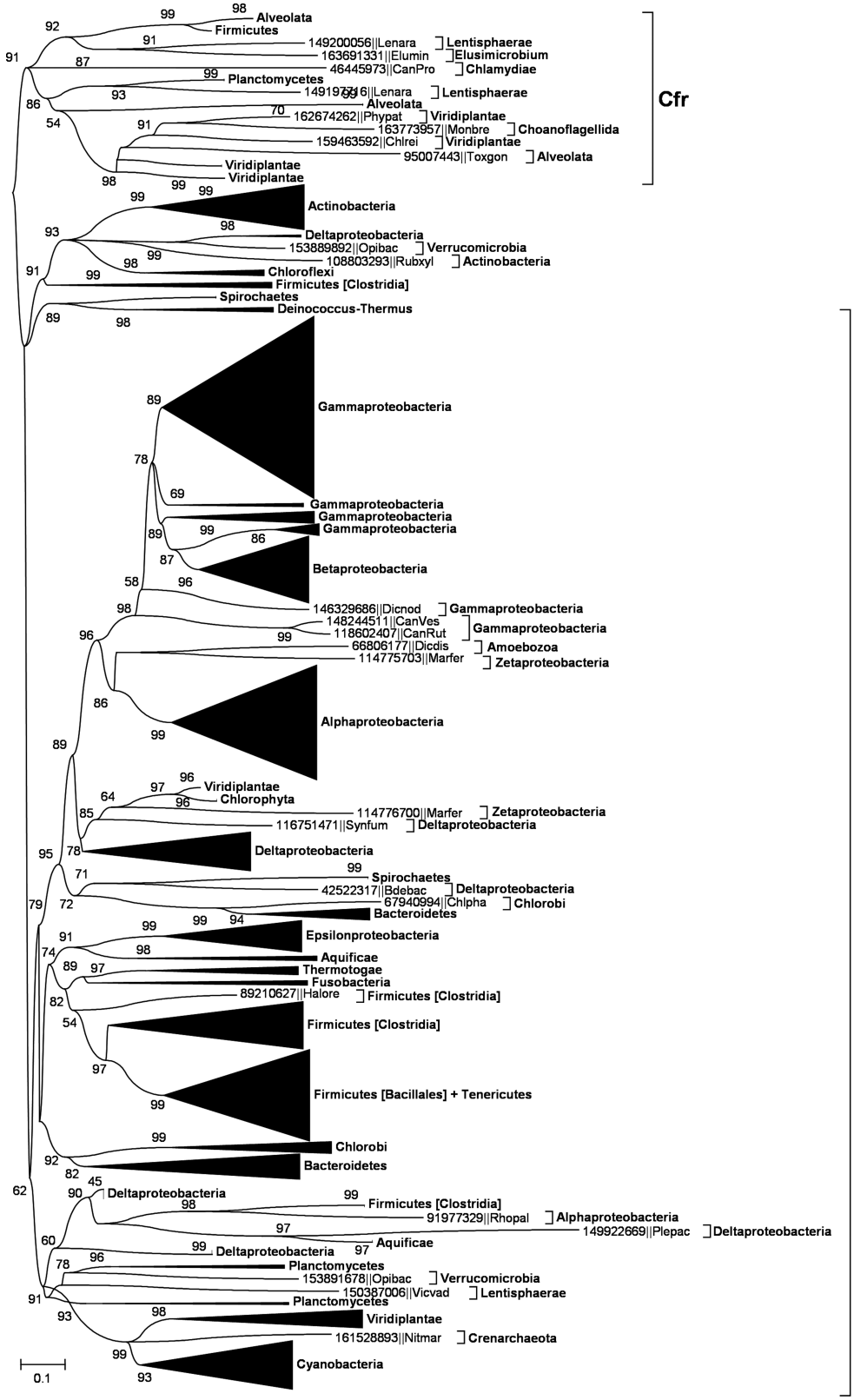

Figure 2. Phylogenetic tree of the Cfr/RlmN family. Branches comprising multiple sequences from the same taxon have been collapsed and are illustrated as triangles marked by the taxon name. Individual sequences are labeled by six-letter abbreviations as described in Figure 1. Bootstrap values are shown for nodes with support of >50%.

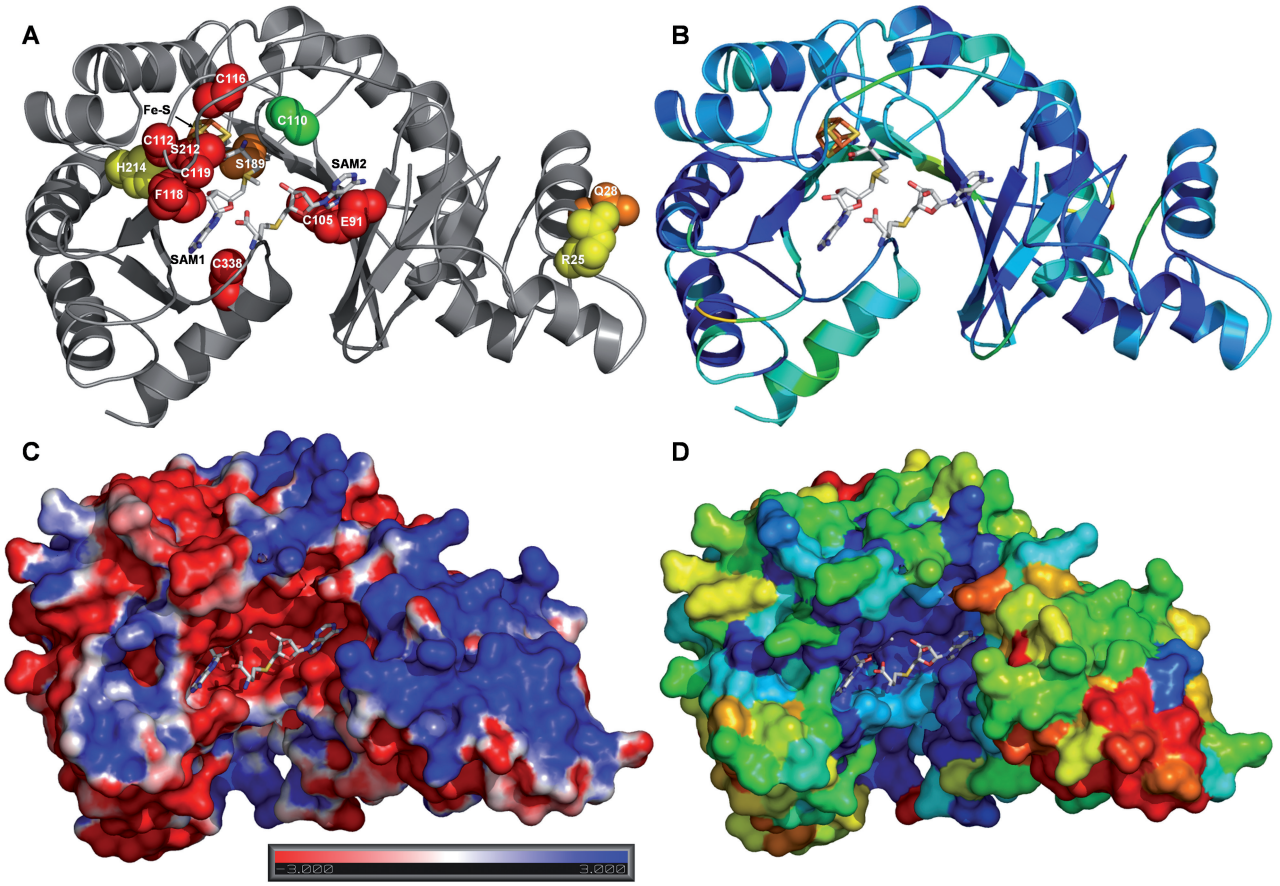

Figure 3. Structural models of the Cfr methyltransferase. The same orientation is shown in all panels, with the N-terminus on the right and C-terminus on the left side. The Fe–S cluster and SAM molecules are colored according to the atom type. The coordinates are available from ftp://genesilico.pl/iamb/models/RadicalSAM/Cfr/. (**A**) The protein backbone is shown in the ribbon representation. Functionally important residues assayed by mutagenesis are labeled and shown in the space-filled representation and colored according to the effect of mutagenesis: red for complete loss of activity, orange for very low activity or yellow for reduced activity. The non-essential residue C110 is indicated in green. (**B**) The Cfr model shown in the ribbon representation, colored according to the predicted error of the model (i.e. the predicted local deviation from the real structure), as calculated by MetaMQAP. Blue indicates low predicted deviation of Cα atoms down to 0 Å, red indicates unreliable regions with deviation >5 Å, green to orange indicate intermediate values. (**C**) The model in surface representation, colored according to the distribution of electrostatic potential, from red (negatively charged) to blue (positively charged). (**D**) The model in the surface representation, colored according to the sequence conservation in the Cfr/RlmN family, from deep blue (invariant), to light blue (conserved), to yellow/red (highly variable).

of 65.8. These results suggest that our model of Cfr is sufficiently reliable as a framework to interpret sequence–function relationships in the Cfr family, at least on the level of amino acid residues. The predicted accuracy of the model is, however, too low for analysis of atomic-level details, docking of ligands by high-resolution *ab initio* methods, and inferring the mechanism of enzymatic reaction by quantum-chemistry methods. Furthermore, the model is probably outside the native energy minimum, and energy minimization is thus not expected to improve its quality.

Prediction of protein–ligand interactions

The binding mode of the 4Fe–4S cluster and the SAM molecule is conserved among all radical-SAM enzymes (34), suggesting that a protein–ligand complex structure can be constructed by using information from homologous proteins. As we consider Cfr to be a radical-SAM MTase, we infer that it needs the 4Fe–4S cluster and the radical-SAM ligands for a radical reaction on C8 in adenosine and an additional SAM as methyl donor. We thus decided to illustrate the potential protein–ligand interactions in Cfr by copying the Fe–S complex and one SAM molecule, hereafter referred to as SAM1, from the molybdenum cofactor biosynthesis protein A complex structure. As MoaA uses only one SAM molecule, the additional SAM molecule (the putative methyl group donor), has been included in our model of Cfr by analogy to the SAM2 molecule in another radical-SAM enzyme, the coproporphyrinogen III oxidase (HemN; PDB code: 1olt). The suggested complex structure of Cfr with the ligands is illustrated in Figure 3. Thus, we infer that residues from the loop comprising the CX_3CX_2C motif and from the third and fourth β-strands coordinate the 4Fe–4S cluster and SAM1, respectively; while residues from the two β-strands that precede the catalytic triad of cysteines and from the last C-terminal helix coordinate the

SAM2 molecule. We must emphasize that the position and orientation of the SAM2 molecule is probably the most speculative aspect of the presented model.

Calculation of the electrostatic potential for the Cfr model (illustrated in Figure 3C) reveals that the surface of the radical-SAM domain is mostly negatively charged, while the NTD exhibits a positively charged surface. Mapping of the sequence alignment onto the protein structure (Figure 3D) shows a concentration of conserved residues both in the radical-SAM domain and to a limited extent also in the NTD, suggesting that both domains are highly relevant for the enzyme function. We hypothesize that the NTD facilitates specific binding to the negatively charged RNA substrate.

Mutagenesis of the Cfr MTase and the effect on methylation activity

Mutations in Cfr were introduced in the *cfr* gene placed after the inducible *lac* promoter and with an N-terminal histidine tag. Each mutation consisted of a single amino acid residue changed to alanine. A few mutations (R25A, Q28A, C338A) have been introduced into the termini of Cfr to determine whether the ends are important for Cfr function. Other mutations have been introduced at amino acids placed at the proposed functional sites for binding of a 4Fe–4S cluster (C112A, C116A, C119A) and two molecules of SAM (SAM1: F118A, S189A, S212A, H214A and SAM2: E91A, C105A). The control mutation C110A was introduced at a position that is conserved in the Cfr/RlmN family, but is neither conserved among radical-SAM enzymes nor makes interactions with ligands in our model and is presumably unimportant.

The activity of the different Cfr mutants was assayed by antibiotic susceptibility testing of a hypersensitive *E. coli* strain (AS19) harboring plasmids expressing the mutant Cfr proteins. The hypersensitive strain facilitates the detection of moderate MIC changes in the Gram-negative bacterium *E. coli*, which is intrinsically resistant to many antibiotics. As expression of wild-type Cfr confers a $PhLOPS_A$ resistance phenotype (3), the antibiotics florfenicol and tiamulin that represent two of the five groups of antibiotics related to this phenotype were chosen for assaying the effect of the mutations. MICs have been determined for strains expressing wild-type and mutant Cfr proteins and the results are presented in Table 1. In addition, various controls without plasmid and with plasmids not containing the *cfr* gene were assayed to assure that the observed effects can be directly attributed to Cfr expression. All the mutations introduced at potential functional sites lowered the MIC values significantly and thus affect Cfr activity. The mutations E91A, C105A, C112A, C116A, C119A, F118A, S212A and C338A eliminate the resistance to both florfenicol and tiamulin, whereas Q28A and S189A lower the resistance considerably and R25A and and H214A yield moderate decreases in MIC values. The C110A control mutation does not affect Cfr activity as the MIC values obtained for this mutant are indistinguishable from those of the wild-type Cfr protein.

Table 1. Antibiotic susceptibilities of *E. coli* AS19 strains with plasmid-encoded *cfr* genes

Plasmid	*cfr* gene	Site of Cfr mutation	FFC MIC (μg/ml)	TIA MIC (μg/ml)
No plasmid	–	n.a.	1–2	2
pBluescript (-Cfr)	–	n.a.	1	1
pLJ102 (-Cfr)	–	n.a.	1	2
pCfrHisR25A	+	NTD	16	8
pCfrHisQ28A	+	NTD	2–4	4
pCfrHisC338A	+	C-terminus	1	2
pCfrHisC112A	+	4Fe-4S	1–2	2
pCfrHisC116A	+	4Fe-4S	1	2
pCfrHisC119A	+	4Fe-4S	1	2
pCfrHisF118A	+	SAM1	1–2	1–2
pCfrHisS189A	+	SAM1	2–4	4
pCfrHisS212A	+	SAM1	2	2
pCfrHisH214A	+	SAM1	16–32	32
pCfrHisE91A	+	SAM2	2	2
pCfrHisC105A	+	SAM2	1	2
pCfrHisC110A	+	Non-conserved	32	>128
pCfrHis	+	None	32	>128
pBglII (+Cfr)	+	None	16–32	128

FFC, florfenicol; TIA, tiamulin; MIC, minimal inhibitory concentration; n.a., not applicable; NTD, N-terminal domain. The 4Fe–4S, SAM1, and SAM2 sites are explained in the Results section.

To further substantiate that the observed MICs are a direct consequence of Cfr activity or lack thereof, position A2503 was assayed for methylation. It has been observed previously that the Cfr-mediated m^8A2503 methylation causes a partial reverse transcriptase stop in primer extension assays (2,3,6). Cfr also represses the YgdE-mediated ribose methylation (36) of C2498 by lowering the intensity of the primer extension stop from this modification (2). Primer extension analysis was performed on total RNA isolated from strains expressing the mutant Cfr proteins. The *E. coli* JW2501-1 strain, that does not contain the RlmN MTase that normally mediates the m^2A2503 modification, was used as the host for plasmids expressing the mutated Cfr proteins and isolation of total RNA. This was done to avoid the weak primer extension stop from the m^2A2503 methylation that overlaps the Cfr-mediated m^8A2503 stop and would therefore interfere with assessment of the activity of the mutated Cfr proteins. The primer extension analysis is presented in Figure 4A.

The C110A control mutation that does not affect MIC values mediates the appearance of a clear strong band at position 2503 by primer extension analysis, indicating a m^8A2503 methylation similar to the wild-type enzyme. For most of the mutants that exhibit changes in MICs relative to wild-type Cfr, analysis of 23S rRNA results in either a weak band or no band at position A2503. This is consistent with an inactivated or partially inactivated Cfr and the decreased MIC values observed for these mutants. The C112A, C116A and C119A mutations of the CX_3CX_2C motif at the presumed 4Fe–4S cluster binding site do not yield any primer extension stop at position A2503, in accordance with a complete inactivation of the Cfr RNA modification activity. The same pattern is seen for the C338A mutation, suggesting a vital importance of this residue. Mutations in the

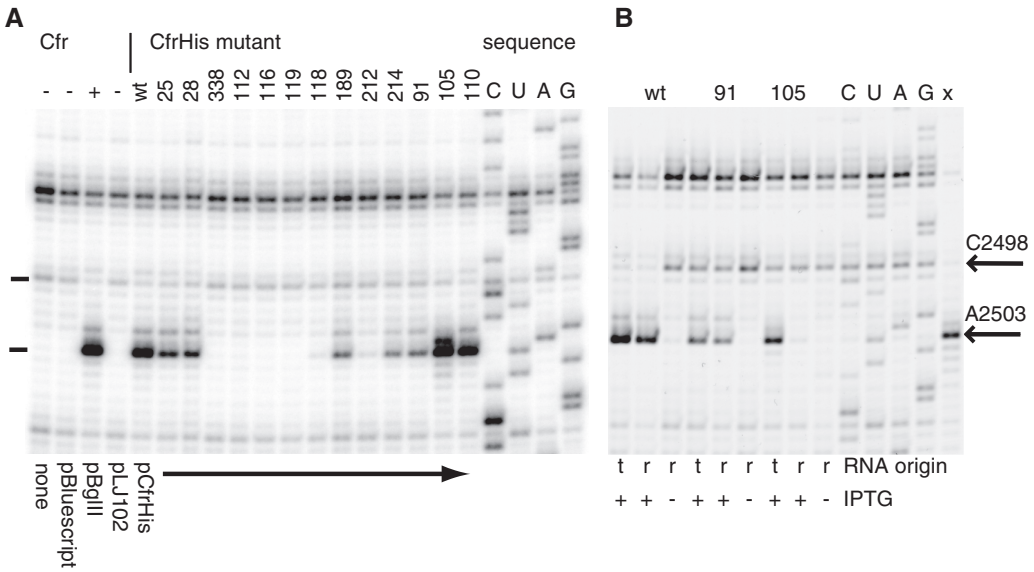

Figure 4. Primer extension analysis of reverse transcriptase stops on 23S RNA from *E. coli* strains harbouring various plasmids expressing Cfr and mutated Cfr or control plasmids. The numbers above the gel correspond to the mutated amino acids (compare with Table 1 for further information). The region shown is limited to the nucleotides flanking A2503 that is methylated by Cfr and C2498 where Cfr inhibits methylation. Lanes marked C, U, A and G refer to dideoxysequencing reactions. Reverse transcriptase stops one nucleotide before the corresponding nucleotide in the sequencing lanes. Panel (**A**) shows primer extension on total RNA from JW2501-1 strains harboring the indicated plasmids. Panel (**B**) shows primer extension on rRNA from isolated 70S ribosomes (r) compared to analysis of total RNA (t) from JW2501-1 strains harboring pCfrHis or mutated plasmids. The rightmost lane marked 'x' shows primer extension analysis of 23S RNA isolated from 50S subunits from mutant C105A (+IPTG). The positions of bands representing A2503 and C2498 are indicated by arrows on the right and horizontal bars on the left. The numbers above the gels refer to the amino acids that have been mutagenized.

predicted SAM1-binding site give rise to a very faint band (F118A and S212A) or a weak band (S189A and H214A), in accordance with nearly background and reduced activities, respectively, also observed with the MIC values. R25A and Q28A mutations in the NTD mediate a band of intermediate intensity, again in good qualitative agreement with the observed intermediate MIC values.

Surprisingly, the E91A and C105A mutations in the predicted SAM2-binding site produce a clear band at the 2503 position despite a sensitive phenotype indicating the absence of methylated and thus antibiotic-resistant ribosomes. A 23S rRNA fragment was isolated from mutant C105A total RNA and MS analysis was performed as previously described for the identification of Cfr as a MTase (2). The MALDI-TOF MS analysis showed no evidence of methylation at position A2503 (data not shown). Thus, the MS data showing no methylation is in agreement with the MICs showing no resistance. We then hypothesized that the band could originate from a fraction of 23S RNA molecules that interacted in an inappropriate way with the mutated Cfr, and as a consequence were not incorporated into functional ribosomes. This was investigated by isolating ribosomes from mutant and control strains and performing primer extension analysis on 23S RNA (shown in Figure 4B). The relative strength of the primer extension stops at A2503 in 23S RNA from mutant E91A is only decreased marginally in the ribosomal RNA samples compared to the total RNA samples. The pattern for mutant C105A is different as the stop is almost absent in RNA from 70S ribosomes. The sucrose gradient from this mutant showed an unusually large 50S fraction and therefore RNA from this peak was also investigated by primer extension (rightmost lane in Figure 4B) and shows a strong stop at the A2503 position. There is thus a selection against the Cfr-affected RNA in purified 70S while this RNA is present in the 50S fraction. Taken together, the data suggest that Cfr mutants E91A and C105A carry out a reaction that results in a primer extension stop, but whose product is not methylated and does not lead to the formation of antibiotic-resistant ribosomes. One possibility is that a portion of 23S rRNA is cleaved or abasic at this position. At present the primer extension band is a mystery that is beyond the scope of the current investigation.

DISCUSSION

Cfr as the founding member of Class VII MTases and its relation to othes MTases

The SAM-dependent MTases have been grouped into five classes that are unrelated in sequence, structure, phylogenetic origin and in the details of protein–SAM interactions (37). A sixth class is represented by a transmembrane protein, isoprenylcysteine carboxyl MTase (ICMTase) (38). A number of other enzyme superfamilies utilize SAM as a cofactor or cosubstrate in various reactions, other than the transfer of the methyl group (39). Among them, the radical-SAM superfamily belongs to the most diverse groups of enzymes, as its members have been found to catalyze reactions such as unusual

methylations, isomerization, sulfur insertion, ring formation, anaerobic oxidation and protein-radical formation (9). This diversity of reactions is reflected in the divergence of sequences and structures among the radical-SAM enzymes compared to other SAM-dependent MTase superfamilies.

There are only few radical-SAM enzymes that catalyze methylation or related reactions. Cfr has been the first experimentally characterized *bona fide* MTase among all radical-SAM enzymes (10), and hence we designate it as the founding member of Class VII SAM-dependent MTases. The radical-SAM enzyme family includes two experimentally characterized MTases BchQ and BchR that are involved in modification of bacteriochlorophyllide *c* at C-8^2 and C-12^1 atoms (40). The MTase CloN6 also belongs to the radical-SAM superfamily and is involved in methylation of the aminocoumarin antibiotic clorobiocin, but this enzyme is believed to use methylcobalamin rather than SAM as the methyl group donor (41). Thus, these enzymes perform reactions that are very different from Cfr methylation and are probably not useful for inferring the mechanism of Cfr methylation.

Other radical-SAM enzymes that target the translational apparatus catalyze thiomethylation reactions. The MiaB enzyme catalyzes thiomethylation of the C-2 atom of N^6-(isopentenyl) adenosine (i^6A)-37 in tRNA (42) and the related RimO enzyme adds a thiomethyl group to the Cβ atom of amino acid residue D88 of ribosomal protein S12 (43). The remote homology of Cfr/RlmN and MiaB is intriguing, given the fact that all three enzymes act on adenosine in RNA and that RlmN and MiaB modify the same C2 atom. MiaB has been postulated to use two molecules of SAM, where SAM1 generates the radical and SAM2 acts as methyl donor (42). Although it was originally proposed that MiaB inserts sulfur from the first SAM molecule, it has recently been shown that this enzyme contains an additional Fe–S cluster, and it has been proposed that this second cluster acts as a sacrificial S-donor (44). We suggest that Cfr uses two SAM molecules like MiaB, where SAM1 is used to generate a highly reactive reaction intermediate, essentially as in all radical-SAM enzymes, while the SAM2 molecule is used as a methyl group donor. The methyl transfer step for Cfr and RlmN might thus be related to the final step of the reactions catalyzed by MiaB and RimO.

Although the structures of RlmN and MiaB are not known, we speculate that they bind the target adenosine residue in a similar manner and use a similar reaction mechanism. It is interesting that Cfr methylates the C-8 atom of adenosine despite its close relationship to RlmN, however Cfr has been found to exhibit latent m^2A MTase activity (6). Based on our phylogenetic analysis we suggest that the C-8 methylation activity is a new invention of Cfr, and that the ancestor of RlmN and Cfr was a m^2A MTase. It is noteworthy that so far no MTases from the more ubiquitous RFM (45) or SPOUT (46) superfamilies have been found to carry out m^2A or m^8A methylation, which probably reflects the challenging chemistry of modification of endocyclic carbon atoms.

Structure-based interpretation of experimental data

Like all theoretical models of protein structure, our model of Cfr is obviously less accurate than typical X-ray crystal and NMR structures but no experimental model of Cfr or any closely related protein is currently available. From the theoretical evaluation by MQAP methods, we consider the current theoretical model to be sufficiently accurate to guide new experimental analyses at the level of individual amino acid residues (e.g. site-directed mutagenesis). For initial experimental testing, we selected a set of residues with functional predictions ranging from obvious (e.g. the Cys motif common to all radical-SAM enzymes) to very non-trivial (residues located in elements that were difficult to model or had no correspondence in other radical-SAM enzymes). The mutagenesis analysis shows that all amino acid residues chosen due to their potential importance actually influence Cfr activity considerably and about half of them completely destroyed the methylation activity (Table 1), implying that they are of high functional importance and presumably positioned in functional sites. As expected, alanine mutagenesis of the invariant residues C112, C116, C119, forming the well-conserved Fe–S cluster-binding motif, completely abolished Cfr function. Interestingly, alanine substitutions of the invariant residue C338 in a Cfr-specific sequence motif 'ACGQL' in the C-terminal helix also caused total inactivation of the enzyme. In our model, this residue is buried in the structure and therefore the effect of the mutation may be due to destabilization of the protein. However, this part of the protein has been constructed *de novo*, so its true conformation may be different, and this Cfr-specific motif could be involved in interactions with the RNA substrate and/or ligands. The effects of mutations in the conserved SAM1-binding site are almost as strong as for the invariant Cys residus, with two mutants (F118A and S121A) showing barely detectable activity and two mutants with weak activity (S189A and H214A). This is in agreement with the relative importance of predicted contacts in the enzyme. According to our model, F118 forms a stacking interaction with the adenosine moiety of SAM1, S212 may interact with the 3′ hydroxyl group of the ribose moiety, while S189 may coordinate the carboxyl group of the methionine moiety. H214 is more distant from SAM1, and may be involved in its long-range coordination. The semi-conserved residues R25 and Q28 are located in the NTD in a part of the molecule unique to the Cfr/RlmN family and predicted to be involved in binding of the substrate RNA. Substitutions at these two positions show only partial loss of activity. Such an effect is analogous to the effect of mutating RNA-binding residues in other RNA MTases, including ErmC′ (47) and Sgm (48). Although not direct evidence, this result is consistent with our prediction of the NTD as an interface for RNA binding by Cfr.

The most interesting mutagenesis effects are observed with residues E91 and C105 located in two β-strands preceding the CX_3CX_2C motif, and predicted to be involved in binding of the SAM2 molecule, the suggested methyl group donor. Accordingly, mutants with alanine substitutions at these positions may show aberrant or no binding

of SAM2. In agreement with this prediction, the antibiotic susceptibility of such mutants is as low as those with mutations in the SAM1-binding site. Nonetheless, these mutant enzymes are carrying out some unknown transformation of the substrate, manifested as a primer extension stop in the product RNA that does not lead to the formation of antibiotic-resistant ribosomes. It could be that E91A and C105A mutants are still capable of binding SAM1 and can initiate the reaction, but cannot finish it without the properly bound SAM2 methyl group donor. This may result in release of a substrate with some form of damage or modification that is manifested as a primer extension stop without leading to antibiotic resistance. These mutants emphasize the functional versatility of radical-SAM enzymes and may be regarded as 'engineered' variants of Cfr with altered reaction mechanisms. Investigation of their activity will be the subject of future studies.

SUPPLEMENTARY DATA

Supplementary Data are available at NAR Online.

ACKNOWLEDGEMENTS

The authors thank Tatjana Kristensen for excellent technical assistance.

FUNDING

JMB acknowledges financial support from grants N301 2396 33 and HISZPANIA/152/2006 from the Polish Ministry of Science and Higher Education. EP acknowledges support from the Foundation for Polish Science (START fellowship). KSL and BV acknowledge financial support from the Danish Medical Research Council and the Danish National Research Foundation. The Open access publication charge for this article has been waived by Oxford University Press. NAR Editorial Board members are entitled to one free paper per year in recognition of their work on behalf of the journal.

Conflict of interest statement. None declared.

REFERENCES

1. Schwarz,S., Werckenthin,C. and Kehrenberg,C. (2000) Identification of a plasmid-borne chloramphenicol-florfenicol resistance gene in *Staphylococcus sciuri*. *Antimicrob. Agents Chemother*., **44**, 2530–2533.
2. Kehrenberg,C., Schwarz,S., Jacobsen,L., Hansen,L.H. and Vester,B. (2005) A new mechanism for chloramphenicol, florfenicol and clindamycin resistance: methylation of 23S ribosomal RNA at A2503. *Mol. Microbiol*., **57**, 1064–1073.
3. Long,K.S., Poehlsgaard,J., Kehrenberg,C., Schwarz,S. and Vester,B. (2006) The Cfr rRNA methyltransferase confers resistance to Phenicols, Lincosamides, Oxazolidinones, Pleuromutilins, and Streptogramin A antibiotics. *Antimicrob. Agents Chemother*., **50**, 2500–2505.
4. Smith,L.K. and Mankin,A.S. (2008) Transcriptional and translational control of the *mlr* operon, which confers resistance to seven classes of protein synthesis inhibitors. *Antimicrob. Agents Chemother*., **52**, 1703–1712.
5. Kehrenberg,C., Cuny,C., Strommenger,B., Schwarz,S. and Witte,W. (2009) Methicillin-resistant and -susceptible *Staphylococcus aureus* strains of clonal lineages ST398 and ST9 from swine carry the multidrug resistance gene *cfr*. *Antimicrob. Agents Chemother*., **53**, 779–781.
6. Giessing,A.M., Jensen,S.S., Rasmussen,A., Hansen,L.H., Gondela,A., Long,K., Vester,B. and Kirpekar,F. (2009) Identification of 8-methyladenosine as the modification catalyzed by the radical SAM methyltransferase Cfr that confers antibiotic resistance in bacteria. *RNA*, **15**, 327–336.
7. Kowalak,J.A., Bruenger,E. and McCloskey,J.A. (1995) Posttranscriptional modification of the central loop of domain V in *Escherichia coli* 23 S ribosomal RNA. *J. Biol. Chem*., **270**, 17758–17764.
8. Toh,S.M., Xiong,L., Bae,T. and Mankin,A.S. (2008) The methyltransferase YfgB/RlmN is responsible for modification of adenosine 2503 in 23S rRNA. *RNA*, **14**, 98–106.
9. Sofia,H.J., Chen,G., Hetzler,B.G., Reyes-Spindola,J.F. and Miller,N.E. (2001) Radical SAM, a novel protein superfamily linking unresolved steps in familiar biosynthetic pathways with radical mechanisms: functional characterization using new analysis and information visualization methods. *Nucleic Acids Res*., **29**, 1097–1106.
10. Wang,S.C. and Frey,P.A. (2007) *S*-adenosylmethionine as an oxidant: the radical SAM superfamily. *Trends Biochem. Sci*., **32**, 101–110.
11. Altschul,S.F., Madden,T.L., Schaffer,A.A., Zhang,J., Zhang,Z., Miller,W. and Lipman,D.J. (1997) Gapped BLAST and PSI-BLAST: a new generation of protein database search programs. *Nucleic Acids Res*., **25**, 3389–3402.
12. Edgar,R.C. (2004) MUSCLE: multiple sequence alignment with high accuracy and high throughput. *Nucleic Acids Res*., **32**, 1792–1797.
13. Tamura,K., Dudley,J., Nei,M. and Kumar,S. (2007) MEGA4: molecular evolutionary genetics analysis (MEGA) software version 4.0. *Mol. Biol. Evol*., **24**, 1596–1599.
14. Kurowski,M.A. and Bujnicki,J.M. (2003) GeneSilico protein structure prediction meta-server. *Nucleic Acids Res*., **31**, 3305–3307.
15. Lundstrom,J., Rychlewski,L., Bujnicki,J. and Elofsson,A. (2001) Pcons: a neural-network-based consensus predictor that improves fold recognition. *Protein Sci*., **10**, 2354–2362.
16. Kosinski,J., Cymerman,I.A., Feder,M., Kurowski,M.A., Sasin,J.M. and Bujnicki,J.M. (2003) A "FRankenstein's monster" approach to comparative modeling: merging the finest fragments of Fold-Recognition models and iterative model refinement aided by 3D structure evaluation. *Proteins*, **53(Suppl. 6)**, 369–379.
17. Kosinski,J., Gajda,M.J., Cymerman,I.A., Kurowski,M.A., Pawlowski,M., Boniecki,M., Obarska,A., Papaj,G., Sroczynska-Obuchowicz,P., Tkaczuk,K.L. *et al*. (2005) FRankenstein becomes a cyborg: the automatic recombination and realignment of fold recognition models in CASP6. *Proteins*, **61(Suppl. 7)**, 106–113.
18. Fiser,A. and Sali,A. (2003) Modeller: generation and refinement of homology-based protein structure models. *Methods Enzymol*., **374**, 461–491.
19. Simons,K.T., Kooperberg,C., Huang,E. and Baker,D. (1997) Assembly of protein tertiary structures from fragments with similar local sequences using simulated annealing and Bayesian scoring functions. *J. Mol. Biol*., **268**, 209–225.
20. Boniecki,M., Rotkiewicz,P., Skolnick,J. and Kolinski,A. (2003) Protein fragment reconstruction using various modeling techniques. *J. Comput. Aided Mol. Des*., **17**, 725–738.
21. Pawlowski,M., Gajda,M.J., Matlak,R. and Bujnicki,J.M. (2008) MetaMQAP: a meta-server for the quality assessment of protein models. *BMC Bioinformatics*, **9**, 403.
22. Wallner,B. and Elofsson,A. (2003) Can correct protein models be identified? *Protein Sci*., **12**, 1073–1086.
23. DeLano,W.L. (2002) *The PyMOL Molecular Graphics System*. DeLano Scientific, Palo Alto, CA, USA.
24. Baker,N.A., Sept,D., Joseph,S., Holst,M.J. and McCammon,J.A. (2001) Electrostatics of nanosystems: application to microtubules and the ribosome. *Proc. Natl Acad. Sci. USA*, **98**, 10037–10041.

25. Sasin,J.M. and Bujnicki,J.M. (2004) COLORADO3D, a web server for the visual analysis of protein structures. *Nucleic Acids Res.*, **32**, W586–W589.
26. Landau,M., Mayrose,I., Rosenberg,Y., Glaser,F., Martz,E., Pupko,T. and Ben-Tal,N. (2005) ConSurf 2005: the projection of evolutionary conservation scores of residues on protein structures. *Nucleic Acids Res.*, **33**, W299–W302.
27. Sambrook,J. and Russell,D.W. (2001) *Molecular Cloning: A Laboratory Manual*, 3rd edn. Cold Spring Harbor Laboratory Press, Cold Spring Harbor, NY.
28. Sekiguchi,M. and Iida,S. (1967) Mutants of Escherichia coli permeable to actinomycin. *Proc. Natl Acad. Sci. USA*, **58**, 2315–2320.
29. Baba,T., Ara,T., Hasegawa,M., Takai,Y., Okumura,Y., Baba,M., Datsenko,K.A., Tomita,M., Wanner,B.L. and Mori,H. (2006) Construction of *Escherichia coli* K-12 in-frame, single-gene knockout mutants: the Keio collection. *Mol. Syst. Biol.*, **2**, 2006.0008.
30. Johansen,S.K., Maus,C.E., Plikaytis,B.B. and Douthwaite,S. (2006) Capreomycin binds across the ribosomal subunit interface using *tlyA*-encoded 2′-O-methylations in 16S and 23S rRNAs. *Mol. Cell*, **23**, 173–182.
31. Stern,S., Moazed,D. and Noller,H.F. (1988) Structural analysis of RNA using chemical and enzymatic probing monitored by primer extension. *Methods Enzymol.*, **164**, 481–489.
32. Wheeler,D.L., Barrett,T., Benson,D.A., Bryant,S.H., Canese,K., Chetvernin,V., Church,D.M., Dicuccio,M., Edgar,R., Federhen,S. *et al.* (2008) Database resources of the National Center for Biotechnology Information. *Nucleic Acids Res.*, **36**, D13–D21.
33. Horton,P., Park,K.J., Obayashi,T., Fujita,N., Harada,H., Adams-Collier,C.J. and Nakai,K. (2007) WoLF PSORT: protein localization predictor. *Nucleic Acids Res.*, **35**, W585–W587.
34. Layer,G., Heinz,D.W., Jahn,D. and Schubert,W.D. (2004) Structure and function of radical SAM enzymes. *Curr. Opin. Chem. Biol.*, **8**, 468–476.
35. Aravind,L., Anantharaman,V., Balaji,S., Babu,M.M. and Iyer,L.M. (2005) The many faces of the helix-turn-helix domain: transcription regulation and beyond. *FEMS Microbiol. Rev.*, **29**, 231–262.
36. Purta,E., O'Connor,M., Bujnicki,J.M. and Douthwaite,S. (2009) YgdE is the 2′-*O*-ribose methyltransferase RlmM specific for nucleotide C2498 in bacterial 23S rRNA. *Mol. Microbiol.*, **72**, 1147–1158.
37. Schubert,H.L., Blumenthal,R.M. and Cheng,X. (2003) Many paths to methyltransfer: a chronicle of convergence. *Trends Biochem. Sci.*, **28**, 329–335.
38. Stephenson,R.C. and Clarke,S. (1992) Characterization of a rat liver protein carboxyl methyltransferase involved in the maturation of proteins with the -CXXX C-terminal sequence motif. *J. Biol. Chem.*, **267**, 13314–13319.
39. Kozbial,P.Z. and Mushegian,A.R. (2005) Natural history of *S*-adenosylmethionine-binding proteins. *BMC Struct Biol.*, **5**, 19.
40. Gomez Maqueo Chew,A., Frigaard,N.U. and Bryant,D.A. (2007) Bacteriochlorophyllide *c* C-8^2 and C-12^1 methyltransferases are essential for adaptation to low light in *Chlorobaculum tepidum*. *J. Bacteriol.*, **189**, 6176–6184.
41. Westrich,L., Heide,L. and Li,S.M. (2003) CloN6, a novel methyltransferase catalysing the methylation of the pyrrole-2-carboxyl moiety of clorobiocin. *Chembiochem.*, **4**, 768–773.
42. Pierrel,F., Douki,T., Fontecave,M. and Atta,M. (2004) MiaB protein is a bifunctional radical-*S*-adenosylmethionine enzyme involved in thiolation and methylation of tRNA. *J. Biol. Chem.*, **279**, 47555–47563.
43. Anton,B.P., Saleh,L., Benner,J.S., Raleigh,E.A., Kasif,S. and Roberts,R.J. (2008) RimO, a MiaB-like enzyme, methylthiolates the universally conserved Asp88 residue of ribosomal protein S12 in *Escherichia coli*. *Proc. Natl Acad. Sci. USA*, **105**, 1826–1831.
44. Hernandez,H.L., Pierrel,F., Elleingand,E., Garcia-Serres,R., Huynh,B.H., Johnson,M.K., Fontecave,M. and Atta,M. (2007) MiaB, a bifunctional radical-*S*-adenosylmethionine enzyme involved in the thiolation and methylation of tRNA, contains two essential [4Fe-4S] clusters. *Biochemistry*, **46**, 5140–5147.
45. Bujnicki,J.M. (1999) Comparison of protein structures reveals monophyletic origin of the AdoMet-dependent methyltransferase family and mechanistic convergence rather than recent differentiation of N^4-cytosine and N^6-adenine DNA methylation. *In Silico Biol.*, **1**, 175–182.
46. Tkaczuk,K.L., Dunin-Horkawicz,S., Purta,E. and Bujnicki,J.M. (2007) Structural and evolutionary bioinformatics of the SPOUT superfamily of methyltransferases. *BMC Bioinformatics*, **8**, 73.
47. Maravic,G., Bujnicki,J.M., Feder,M., Pongor,S. and Flogel,M. (2003) Alanine-scanning mutagenesis of the predicted rRNA-binding domain of ErmC' redefines the substrate-binding site and suggests a model for protein-RNA interactions. *Nucleic Acids Res.*, **31**, 4941–4949.
48. Maravic Vlahovicek,G., Cubrilo,S., Tkaczuk,K.L. and Bujnicki,J.M. (2008) Modeling and experimental analyses reveal a two-domain structure and amino acids important for the activity of aminoglycoside resistance methyltransferase Sgm. *Biochim. Biophys. Acta*, **1784**, 582–590.